Preserving Synchronization Accuracy from the Plug-in of NonSynchronized Nodes in a Wireless Sensor Network

Preserving Synchronization Accuracy From the Plug-in of NonSynchronized Nodes in a Wireless Sensor Network

Francesco Lamonaca, *Senior Member, IEEE*, Domenico Luca Carnì, *Member, IEEE*, Maria Riccio, *Senior Member, IEEE*, Domenico Grimaldi, *Senior Member, IEEE*, and Gregorio Andria, *Member, IEEE*

***Abstract*— The synchronization accuracy of the nodes of a wireless sensor network (WSN) can be perturbed by the plug-in of nonsynchronized nodes (NSNs). In the case of peer-to-peer synchronization algorithms, the reference time of the WSN is established on the basis of the clock time of all nodes. Therefore, each NSN changes the reference time to synchronize all nodes with the new reference time interval needs. In this time interval, the synchronization accuracy can degrade, i.e., the delay among node clocks overcomes the admissible range.**

In the case of only one or many NSNs, it was assessed in previous papers that by filtering the message of each NSN, the synchronization accuracy of the already synchronized nodes (ASNs) is preserved. However, the spatial distribution of the NSNs can fool the ASNs, foiling the effect of the message filtering. This paper presents a procedure that overcomes this inconvenience. The new fully distributed and consensus-based procedure iteratively filters the messages of communicating NSNs that would increase the time delay over the admissible range. As a consequence, the synchronization accuracy is preserved whatever the spatial distribution of ASNs and NSNs. Numerical and experimental tests are performed to validate the proposed procedure.

***Index Terms*— Consensus, synchronization, wireless sensor network (WSN).**

I. Introduction

WIRELESS sensor networks (WSNs) are large-scale networks of small, low-cost, and low-power wireless sensors dedicated to observing and monitoring physical systems [1]–[5]. The time synchronization among nodes is usually performed by an algorithm based on the periodic exchange of messages among nodes containing their time values.
The required synchronization accuracy is determined
by the dynamic of the system under monitoring [6]–[10] and it must be guaranteed during all the working operations that can occur.

The degradation of synchronization accuracy can be caused by the exchange of messages containing time values increasing the standard deviation of the time delay among nodes over the required synchronization accuracy.

In the paper, the effect of this cause is analyzed by referring to peer-to-peer synchronization algorithms [11]–[14]. These algorithms are based on the sharing of synchronization messages among the interacting nodes in order to establish the virtual time of the network. This is unknown to all nodes, but it is the reference time of all nodes [15]. As shown in [16] and reported in [15], [17], and [18] the peer-to-peer synchronization approaches need the network to be connected, i.e., there is a communication path between any couple of nodes. This condition is also required by other message-based synchronization algorithms presented in the recent lit-erature [19]. Indeed, if this condition is not satisfied there is at least one node that cannot exchange synchronization messages with each node, and as a consequence, it cannot be synchronized.

In the case of the plugging of nonsynchronized nodes (NSNs), the synchronization accuracy would degrade temporarily because the virtual time is established on the basis of the time values of all the WSN nodes. The synchronization accuracy degradation can provoke delays among node clocks over the admissible range, causing errors in the evaluation of the dynamic of the system under monitoring [20]–[24]. Preserving synchronization accuracy imposes that the time delay among already synchronized nodes (ASNs) is always constrained in the admissible range.

In [25], a consensus-based procedure was proposed to preserve synchronization accuracy in the case of the plug-in of one NSN. Each node detects and filters the information sent by the NSN. The detection is based on the comparison among the time values exchanged through the synchronization messages. Consequently, each node synchronizes its clock on the basis of the time values of the ASNs and the WSN virtual time does not change. As a consequence, the NSN is forced to converge to the WSN virtual time.

In [17], the plug-in of multiple NSNs is taken into consideration and the detection and filtering action was extended to messages coming from many NSNs. The result is that the synchronization accuracy is preserved in the time domain, i.e., it does not change after the plug-in of the NSNs.

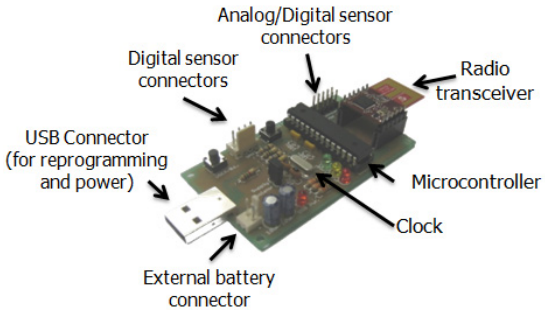

Fig. 1. Hardware structure of a WSN node.

However, the spatial distribution of NSNs can foil the effect of the filtering because the ASNs receive many messages from NSNs misstating the procedure to distinguish among ASN and NSN messages.

In order to overcome this inconvenience, this paper points out a proper filtering procedure to preserve synchronization accuracy whatever the spatial distribution of NSNs and ASNs. As an extension of [17], the proposed procedure uses the probabilistic approach to filter the messages coming from NSNs. Different from [17], the procedure iteratively searches and rejects the NSN messages to minimize the standard deviation of the received time values until it becomes lower than the required synchronization accuracy. This approach allows filtering of the NSN messages regardless of their spatial distribution.

The paper is organized as follows: the proposed filtering and synchronizing procedure is presented in Section II; the software structure of the WSN node supporting the proposed procedure is introduced in Section III; the numerical validation tests are presented in Section IV; the experimental results are presented in Section V; the conclusion follows.

II. Filtering and Synchronizing Procedure

The hardware structure of a wireless sensor, which is the node of the WSN and available on the market allowing the synchronization service, is shown in Fig. 1. It is equipped with a nontunable hardware clock, typically made by a crystal oscillator and a counter.

The number of clock impulses of the hardware clock $\tau_i(t)$ of the ith node, Node#i, at time t is

$$\tau_i(t) = \lfloor \alpha_i t \rfloor + \beta_i, \quad i = 1, \ldots, N_c \tag{1}$$

where $\lfloor \cdot \rfloor$ is the floor operator, N_c is the number of nodes, α_i is the frequency and β_i the offset of the clock.

Owing to the actual creation of the clock and the different operative conditions of the nodes, the couples (α_i, β_i) are slightly different in the nodes.

The synchronization procedure operates on the software clock $\hat{\tau}_i(t)$

$$\hat{\tau}_i(t) = \hat{\alpha}_i(t)\tau_i(t) + \hat{o}_i(t) \tag{2}$$

where the correction parameters $\hat{\alpha}_i(t)$, and $\hat{o}_i(t)$ are evaluated according to the block scheme of Fig. 2, on the basis of synchronization messages exchanged among the communicating nodes.

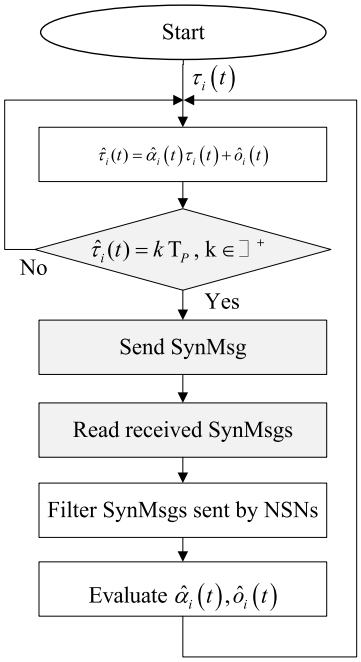

Fig. 2. Block scheme of the synchronization procedure executed in each node of the WSN.

The synchronization procedure works under the hypothesis as follows.

1) Each node exchanges synchronization messages, in broadcast modality, with period T_p, i.e., $t_k = kT_P$, $k \in \mathbb{N}^+$, where $\mathbb{N}^+$ is the set of natural numbers without zero. This hypothesis allows energy to be saved since it reduces the number of synchronization messages to be transmitted with respect to the case of the multiple sending modality.
2) There is a communication path between any couple of nodes. Otherwise, there is not one but many WSNs that do not communicate, and it is not possible to synchronize them with the synchronization methods based on message passing [18], [19]. A solution is to use the synchronizing embedded hardware proposed in [26] to bring the sense of time of one WSN to another.
3) Each node has a unique identifier. This hypothesis permits the implementation of a communication policy preventing the loss of synchronization messages. The unique identifier is assigned to the node by the network designer during the programming step.

The message SynMsg_{ji}, sent at t_k by Node#j is received by Node#i after the random delay $\Delta\ t_{ji}(t_k)$ introduced by the hardware and software path connecting the clock, the microcontroller, and the radio transceiver of Node#i and Node#j. SynMsg_{ji}, includes: id_j, $\hat{\alpha}_j(t_k)$, $\hat{o}_j(t_k)$, $\tau_j(t_k)$, where id_j is the node identifier.

At reception of the SynMsg_{ji}, the Node#i stores in the jth row of the matrix M_i the number of clock impulses at the reception τ_{ij} and the parameters included in SynMsg_{ji}. Moreover, M_i includes two adjunctive columns: row j stores τ_j^{old} and τ_{ij}^{old}, that refers to the previous reception of SynMsg_{ji}. It is worth noting that, owing to packet loss, it can occur that one or more messages sent by node j are not received by Node#i.

If $\Delta t_{ji}(t_k)$ is negligible with respect to the clock period, it is $\tau_{ij} = \tau_i(t_k)$, otherwise $\Delta t_{ji}(t_k)$ must be compensated [27].

In order to prevent the loss of SynMsgs due to simultaneous transmission, and to permit the use of standard hardware not allowing the simultaneous transmission and reception of messages, the following procedure based on time division multiple access policy is adopted. At $t_k = kT_P$, $k \in \mathbb{N}^+$ Node#j, $j = 1 \ldots N$, before sending, SynMsg waits a time interval $\Delta t_{\text{wait},j} = id_j * \Delta t_{\text{wait}}$, where Δt_{wait} is the time interval established in the design of the network. As a consequence, $\Delta t_{\text{wait},j}$ is different $\forall j$ and the loss of SynMsgs is prevented. Since Node#j sends id_j by SynMsg, the receiving nodes are able to compute $\Delta t_{\text{wait},j}$ and to compensate it.

A. Filtering of Synchronization Message From NSNs

Let $I(t_k)$ be the set of synchronization messages received by Node#i, in the time interval $[t_k - \delta t; t_k + \delta t]$, with δt according to the synchronization accuracy among nodes. Owing to packet loss, the cardinality of I, $|I(t_k)|$ could vary in the range [1,…,L_i] where L_i is the number of nodes communicating with Node#i. It is mandatory that Node#i receives at least one message to execute the synchronization procedure. Node#i computes the standard deviation $\sigma_i(t)$ of the $\hat{\tau}_j(t)$, $j = 1 \ldots |I(t_k)|$. Two conditions occur as follows.

1) $\sigma_i(t) \leq \sigma_S$*:* the standard deviation of the received time values is lower than the one required by the monitoring application. As a consequence, Node#i accepts all the synchronization messages for the evaluation of $\hat{\alpha}_j(t_k)$ and $\hat{o}_j(t_k)$.
2) $\sigma_i(t) > \sigma_S$*:* the standard deviation of the received time values is greater than the one required by the monitoring application. This condition can occur if at least one synchronization message sent from an NSN is received. If this condition occurs at the startup of the WSN, Node#i accepts all the received synchronization messages. Otherwise, Node#i filters the synchronization messages from NSNs.

The synchronization message maximizing the standard deviation of the received time values is iteratively detected and removed from $I(t_k)$. In particular, $\text{SynMsg}_{\text{ri}}$, with $r = 1, \ldots, |I(t_k)|$, is removed from $I(t_k)$ on the basis of the following condition:

$$r = \min_j(\sigma(I(t_k) \backslash \{\text{SynMsg\#}j\})) \quad \forall j = 1, \ldots, |I(t_k)|. \tag{3}$$

If $\sigma_i(t) > \sigma_S$, there is in $I(t_k)$ another synchronization message sent from NSN that must be removed. Once $\sigma_i(t) \leq \sigma_S$, the messages remaining in $I(t_k)$ constitute the subset $I_h(t_k)$ of synchronization messages sent from ASNs, only.

If $|I_h(t_k)| > \lceil |I(t_k)|/2 \rceil$, i.e., if the number of synchronization messages from ASNs is greater than half of the total number of received messages, then it is assumed that the WSN is not at the startup, and the synchronization messages belonging to $I_h(t_k)$ are used to synchronize. If the WSN is at the startup, the synchronization messages belonging to $I(t_k)$, i.e., all the received messages, are used to synchronize.

The detection uses the *a priori* knowledge of the settling time of the WSN, i.e., the time elapsed from the start of the WSN to the time at which the WSN parameters, including the delay among nodes, enter and remain within the admissible range. If a node detects the condition $|I_h(t_k)| \leq \lceil |I(t_k)|/2 \rceil$ for a time greater than the settling time of the WSN, it means that synchronization procedure does not work and an alarm is generated. Furthermore, since all nodes execute the proposed filtering procedure, the NSNs synchronize only by considering the ASNs message. The time interval to synchronize (Δ_{TIS}), i.e., the time interval starting with the plug-in of the NSNs and ending when the delay between any couple of nodes is in the admissible delay range, with the proposed procedure is lower with respect to the one obtained without the proposed procedure.

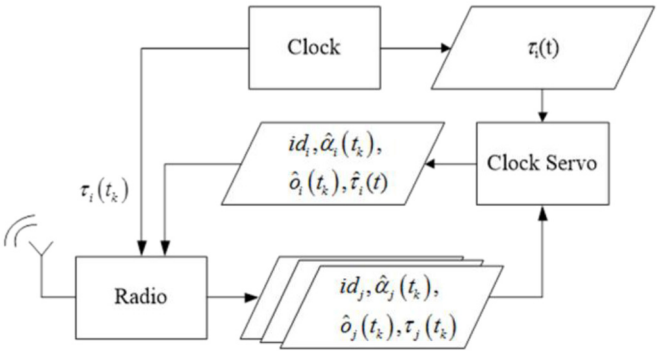

Fig. 3. Block scheme of the software structure of the node:in box the threads, and in parallelogram the shared variables.

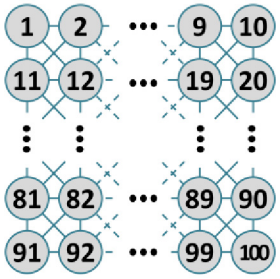

Fig. 4. Lattice topology [10 × 10] nodes.

B. Frequency and Offset Correction

Once the messages coming from NSNs are filtered as in Section II-A, the following two steps are performed.

$\hat{\alpha}_i(t_k)$ is updated according to

$$\hat{\alpha}_i(t_k^+) = \rho_v \hat{\alpha}_i(t_k) + (1 - \rho_v) \frac{\tau_j - \tau_j^{\text{old}}}{\tau_{ij} - \tau_{ij}^{\text{old}}} \hat{\alpha}_j(t_k) \tag{4}$$

where ρ_v is the design parameter set in the interval $0 < \rho_v < 1$ [15], $\hat{\alpha}_i(t_k) = 1$ for $t_k = 0$, and $i = 1 \ldots N$. A higher value of ρ_v causes a wider convergence time interval but reduces the effect of noise in the tuning.

$\hat{o}_i(t_k)$ is updated according to

$$\begin{aligned} \hat{o}_i(t_k^+) = \hat{o}_i(t_k) + (1 - \rho_o)(\hat{\tau}_j(t_k) - \hat{\tau}_i(t_k)) \\ - (\hat{\alpha}_i(t_k^+) - \hat{\alpha}_i(t_k))\tau(t_k) \end{aligned} \tag{5}$$

where ρ_o is the design parameter set in the interval $0 < \rho_o < 1$ [15], $\hat{o}_i(t_k) = 0$ for $t_k = 0$, and $i = 1, \ldots, N$.

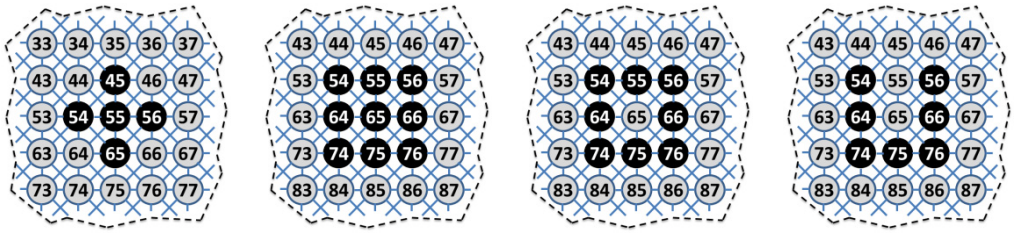

Fig. 5. Spatial distributions of the NSNs, black dots.

A higher value of ρ_o causes a wider convergence time interval but reduces the effect of noise in the tuning.

It is worth noting the following.

1) Since the evaluation of $\hat{\alpha}_i(t_k)$ depends on τ_j^{old} and τ_{ij}^{old}, $\hat{\alpha}_i(t_k)$ can be evaluated after the second exchange of synchronization messages, i.e.,$t_k \geq 2T_P$.
2) Because τ_j^{old} and τ_{ij}^{old} are stored in the node, the evaluation of $\hat{\alpha}_i(t_k)$ can be performed also in the case of packet loss as demonstrated in [15]. Indeed, $\hat{\alpha}_i(t_k)$ is evaluated on the basis of the variation of the clock time values at Node#i and Node#j on the time interval ΔT_{ev}. If there is no packet loss, $\Delta T_{ev} = T_P$. If there are q consecutive packet losses from Node#j to Node#i, $\Delta T_{ev} = qT_P$.
3) the iterative procedure to filter the NSNs messages does not influence the convergence property of the synchronization procedure because the filtering can be considered as a cause of packet loss and then it falls in the previous case.

III. Software Structure of WSNs Node

The software architecture of the node is designed according to the hardware architecture of sensors available on the market (Fig. 1) taking into account the components involved in the synchronization process. The software architecture is made up of three threads: Clock, Clock Servo, and Radio (Fig. 3). They implement the behavior of the clock, microcontroller, and radio transceiver that operate independently. The interaction among threads is achieved by sharing the variables: $\tau_i(t)$, $\hat{\tau}_i(t)$, and the parameters received in the synchronization messages [17].

The values α_i and β_i, are initialized with random values drawn from a statistical distribution representing the characteristics of the hardware clock typically equipping a commercial WSN node.

At each step, the Clock upgrades $\tau_i(t)$ according to (2), and by adding a random value n_s representing the effect of the clock signal noise.

The Clock Servo implements the synchronization procedure and, at each T_P, it: 1) sends in broadcast the synchronization message; 2) reads the messages received from the connected nodes; 3) filters the messages coming from NSNs; 4) evaluates the new values of the correction factors; and 5) update $\hat{\tau}_i(t)$ [13], according to (2).

At time interval T_O, the Clock Servo thread sends to a daemon service a message containing the parameters id_i and $\hat{\tau}_i(t)$. The daemon stores the service message to permit the post analysis of the trend of the delay among the nodes. In order to monitor the trend of the delay among nodes in T_P and after each synchronization, T_P is imposed as a multiple of T_O.

The Radio thread: 1) receives the synchronization messages from the other nodes and 2) broadcasts the synchronization messages received by the Clock Servo.

IV. Numerical Tests

The numerical tests in [8], [17], and [29] were strongly related to the experimental results. This highlights the possibility of using the software architecture and parameter setting for property analysis using simulation, down to real execution. Therefore, no changes are introduced to the software architecture, and the same simulation settings and data are used here.

The only difference is that the Clock Servo implements the filtering of synchronization messages from NSNs.

As in [8], [17], and [29], the parameters for the execution of the numerical tests are selected according to the TelosB node. In particular, according to the characteristics of the crystal oscillator equipping TelosB is $T_{\text{clk}} = 1$ ms, α_i varies uniformly in the range [0.999 980, 1.000 020] kHz; n_s is drawn from a normal distribution with standard deviation of 0.0028 T_{clk}; β_i, is determined by the startup delay of the nodes. In the tests, the case of nodes powered together is considered, for example by powering all of them by USB strip, β_i, varies in the range [0, 300] T_{clk}. T_p is set to 10 s in order to execute many synchronization steps in a reduced experimental observation time. T_O is set to 2 s in order to monitor the delay among nodes during T_p and after each synchronization.

The lattice topology of the WSN is selected because it is typically used in WSN for measurement applications [13], [14], and allows [30], [31]: 1) repeatability of the tests; 2) simultaneous data transmission from different nodes; and 3) alternative path in case a node fails.

The lattice topology of 10 × 10 nodes (Fig. 4) is taken into examination, and the delay among all nodes and Node#100 assumed as reference is considered. It is worth noting that the selection of a different reference node just adds an offset in the trend of the delay among nodes, but does not alter the statistical properties of the delay.

The NSNs are plugged-in 3000 s after the synchronization of the ASNs is achieved. It is assumed that the synchronization is achieved if the delay among any couple of nodes varies in the admissible range equal to $30T_{\text{clk}}$ corresponding to $3\sigma_s$. The admissible range is selected according to the σ_s required in some monitoring applications [32]–[34].

TABLE I

TREND OF THE DELAY REFERRED TO THE SPATIAL DISTRIBUTIONS OF FIG. 5

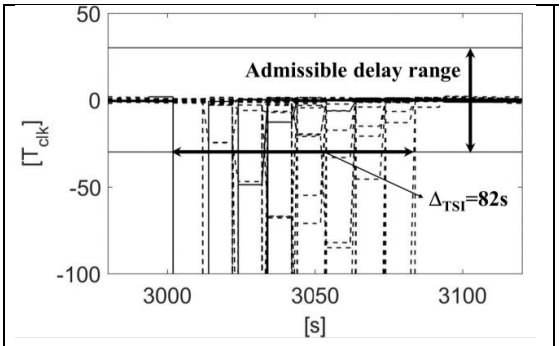	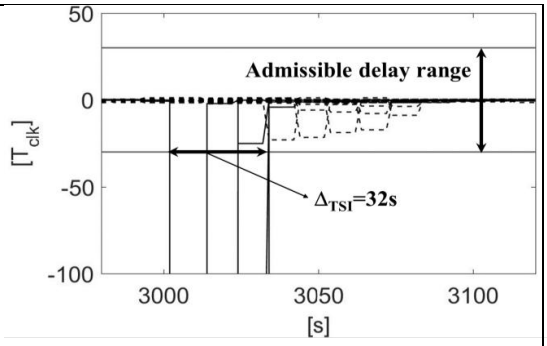
SPATIAL DISTRIBUTION OF FIG.5 (a) WITHOUT PROPOSED PROCEDURE	SPATIAL DISTRIBUTION OF FIG.5 (a) WITH PROPOSED PROCEDURE
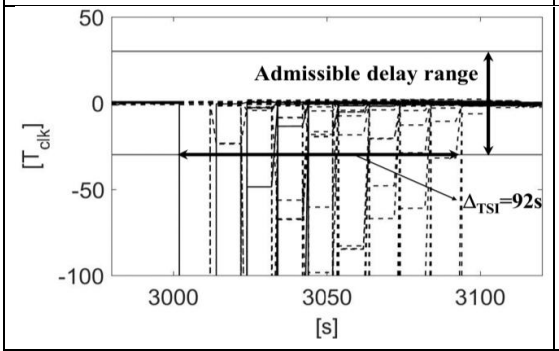	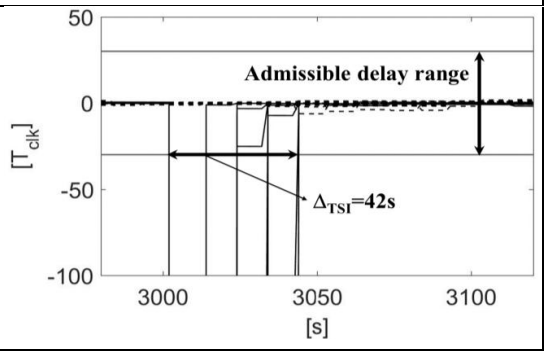
SPATIAL DISTRIBUTION OF FIG.5 (b) WITHOUT PROPOSED PROCEDURE	SPATIAL DISTRIBUTION OF FIG.5 (b) WITH PROPOSED PROCEDURE
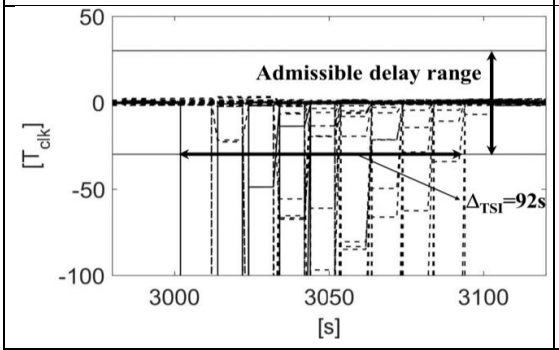	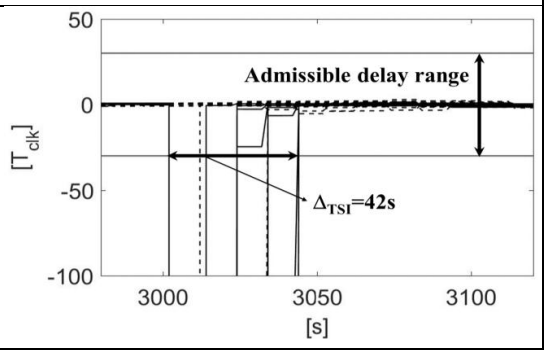
SPATIAL DISTRIBUTION OF FIG.5 (c) WITHOUT PROPOSED PROCEDURE	SPATIAL DISTRIBUTION OF FIG.5 (c) WITH PROPOSED PROCEDURE
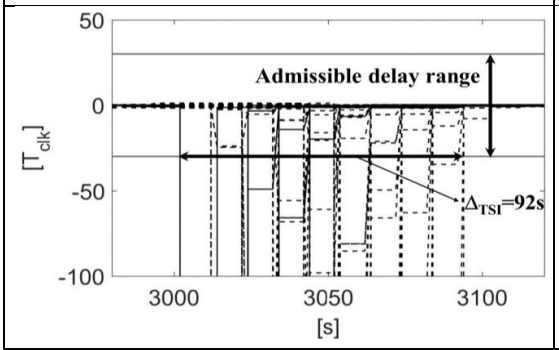	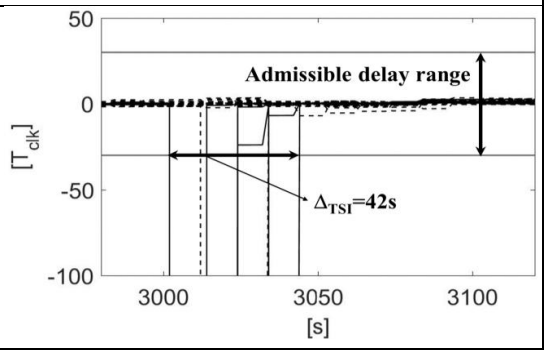
SPATIAL DISTRIBUTION OF FIG.5 (d) WITHOUT PROPOSED PROCEDURE	SPATIAL DISTRIBUTION OF FIG.5 (d) WITH PROPOSED PROCEDURE

Four tests are executed by considering the spatial distribution of the NSNs' topologies, denoted by black nodes, as shown in Fig. 5.

The spatial distributions of the NSNs in Fig. 5 are selected because they are basic distributions and more complex ones can be obtained by combing them.

Table I shows for each test: the trend of the time delay among nodes and Node#100 without and with the use of the proposed procedure to filter the synchronization message from NSNs. The trend of the delay of the NSNs is depicted in black bold lines.

In the case the proposed procedure is not used, the synchronization accuracy among ASNs is not preserved: the time delay among ASNs overcomes the admissible range. In the case the proposed procedure is used, the synchronization accuracy among ASNs is preserved and the NSNs converge to

TABLE II

SYNCHRONIZATION PERFORMANCES FOR FULLY CONNECTED TOPOLOGY

		Without the proposed procedure		With the proposed procedure	
Percentage of NSNs	*Topology of NSNs*	*Perturbs at least one ASN*	*Time interval to synchronize [s]*	*Perturbs at least one ASN*	*Time interval to synchronize [s]*
5	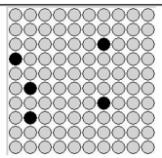	YES	122 ±12	NO	272±12
10	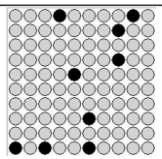	YES	832±12	NO	240±12
20	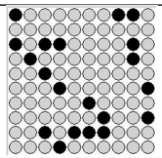	YES	1292±12	NO	272±12
40	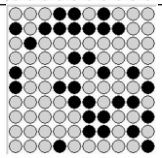	YES	1492±12	NO	320±12
60	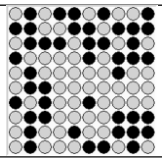	YES	1540±12	YES	310±12
80	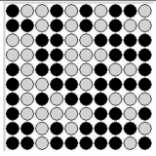	YES	1738±12	YES	270±12

the reference time established on the basis of the clock time values of the ASNs.

Moreover, the value of Δ_{TIS} is shown in Table I for each test.

In Test#1 and #2 the ASN is almost connected with 3 NSNs and 5 ASNs. In the two tests, the synchronization accuracy among ASNs is preserved only with the use of the proposed filtering procedure.

In Test#3, Node#65 is connected only with NSNs. With the proposed procedure, only Node#65 degrades the synchronization accuracy while the other ASNs preserve it. Without the proposed procedure all the ASNs degrade the synchronization accuracy.

In Test#4, Node#65 is connected with 7 NSNs and one ASN, Node#55 is connected with 4 NSNs and 4 ASNs. With the proposed procedure, only Node#65 degrades the synchronization accuracy while the other ASNs preserve it. Without the proposed procedure all the ASNs degrade the synchronization accuracy.

In all the tests, the time interval to synchronize the WSN with the proposed procedure is reduced more than the 50% with respect to the case when it is not used. This is justified by the fact that each NSN executes the same synchronization procedure of the ASNs and, as consequence, each NSN excludes its own value from $I(t_k)$ and computes $\hat{\alpha}_j(t_k)$ and $\hat{o}_j(t_k)$ only on the basis of the ASNs. The final effects are: 1) the NSN does not influence the ASNs because its message is ignored and 2) the ASNs have strong influence on the NSN speeding-up its convergence to the reference time.

Further tests are executed by considering fully connected topology and different percentages of NSNs plugged in. Owing to full connectivity of the NSNs, the distribution of the nodes does not have an influence on the synchronization accuracy. As a consequence, these tests furnish indications to know whether the selected spatial distribution of NSNs with respect to that of ASNs perturbs the ASNs synchronization accuracy.

The spatial distribution of NSNs is randomly selected. As shown in Table II, with the proposed procedure the synchronization accuracy of the ASNs is not perturbed until 60% of the NSNs are plugged in. Without the proposed procedure, the plug in of 5% of the NSNs degrades the synchronization accuracy of the ASNs. Moreover, it can be noted that the time

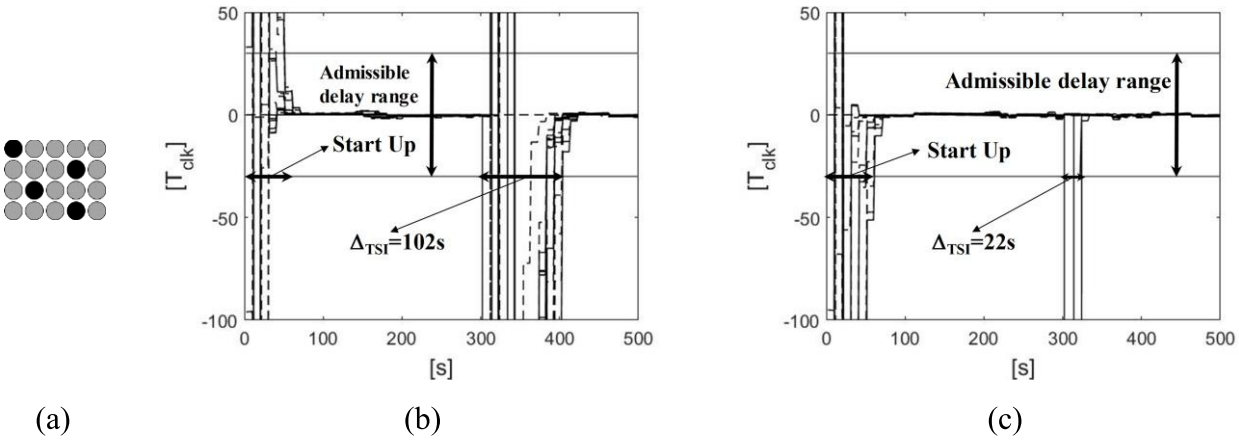

Fig. 6. (a) Distribution of NSNs (black nodes). Trend of the delay of the NSNs (black line), and ASN (gray line), with respect to Node#1 (b) without and (c) with the proposed procedure.

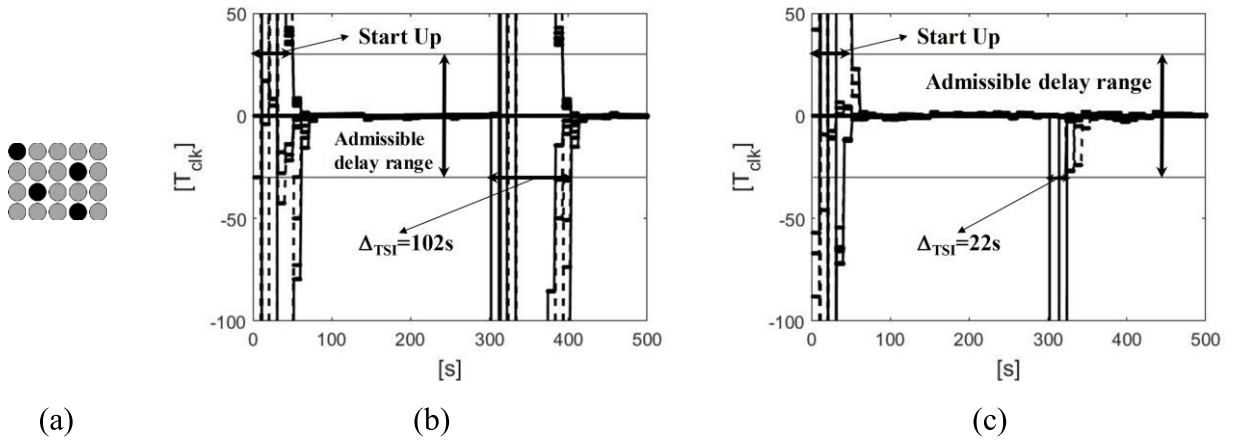

Fig. 7. (a) Distribution of NSNs (black nodes). Trend of the delay of the NSNs (black line), and ASN (gray line), with respect to the first received time value sent by an ASN (b) without and (c) with the proposed procedure.

interval required by the WSN to synchronize after the plug-in of NSNs is determined by the number of NSNs in the case the proposed procedure is not used, while it is independent in the case the proposed procedure is used. Δ_{TIS} is evaluated with resolution of $T_O = 2$ s. The variability of Δ_{TIS} is determined by the synchronization period $T_P = 10$ s. Indeed, in the case some NSNs are added before t_k, they start to synchronize at t_k, the others at at $t_{k+1} = t_k + T_p$ [35]. As a consequence, the maximum variability of Δ_{TIS} is of 12 s.

In order to evaluate the influence of the clock noise on Δ_{TIS}, further numerical tests are executed taking into account 20 nodes in lattice topology. Different topologies and percentages of NSNs are taken into examination. Each test is repeated 30 times. All the NSNs are added after t_k, with $k = 30$. Fig. 6(a) shows the spatial distribution of the NSNs, denoted by black nodes; and Fig. 6(b) and (c) shows the trend of the time delay among nodes and Node#1 without and with, respectively, the proposed procedure to filter the synchronization message from NSNs. The trend of the delay of the NSNs is depicted in black bold lines.

Without the filtering, synchronization accuracy is not preserved. In particular, the time delay among ASNs overcomes the admissible range. With the proposed filtering procedure, the synchronization accuracy is preserved. In particular, the NSNs converge to the reference time established on the basis of the clock time values of the ASNs.

For each percentage of NSNs plugged in, the numerical results showed a negligible influence of the clock noise on Δ_{TIS}. This is justified by the fact that, according to the theory [15], [16], the synchronization accuracy improves each t_k, i.e., every $T_P = 10$ s. As a consequence, Δ_{TIS} is a multiple of T_P and is evaluated with accuracy equal to sampling period $T_O = 2$ s.

V. Experimental Results

Experiments were carried out to evaluate the proposed framework. The WSN is composed of 20 nodes deployed in less than one square meter. The lattice topology is implemented by forcing each node to ignore messages sent by nodes which are not considered as neighbors. The high density of node per square meter allows the evaluation of the effectiveness of the proposal in a saturated spectrum network. Each node is made up of a TelosB wireless sensor [36], allowing the MAC-layer timestamping and then reducing potential

unpredictable delays between the readings and the transmitting of the synchronization messages. The experimental testbed is implemented as in [8] and [27]. In particular, it is set $T_P = 10$ s, $T_O = 2$ s and $\Delta t_{\text{wait}} = 50$ ms, so that each node can receive all the SynMsgs within T_O.

By referring to the distribution of NSNs of Fig. 7(a), Fig. 7(b) shows the trend of the delay without the proposed procedure. The synchronization accuracy is not preserved and the time delay among ASNs overcomes the admissible range. Fig. 7(c) shows the trend of the delay with the proposed procedure. The synchronization accuracy is preserved and the NSNs converge to the reference time established on the basis of the clock time values of the ASNs.

By comparing the numerical results (Fig. 6) with the experimental ones (Fig. 7) a similar trend of the delay and the same node behaviors can be noticed. Without the proposed procedure $\Delta_{\text{TIS}=}$ 102 s both in case of numerical [Fig. 6(a)] and experimental tests [Fig. 7(a)]. With the proposed procedure the value of $\Delta_{\text{TIS}=}$ 22 s both in the case of numerical [Fig. 6(b)] and experimental tests [Fig. 7(b)].

VI. Conclusion

The paper takes into account the WSN synchronization in the case more than one NSN are plugged-in. The effect of spatial distributions of the NSNs is analyzed.

The plug-in of NSNs in the already synchronized WSN can degrade the synchronization accuracy in an unpredictable way because a new reference time is imposed.

The aim of the paper is to constrain the synchronization accuracy in the admissible range in both the time and space domain: after the plug-in of multiple NSNs and whatever their spatial distribution. To this aim, a completely decentralized procedure is proposed allowing each ASN to filter the NSN messages iteratively. The effect of the filtering is that the ASN update the correction parameters on the basis of the ASNs messages only. As a consequence, the synchronization accuracy among ASNs is always constrained in the admissible range. Moreover, because the proposed procedure is executed also by NSNs, they speed up the convergence to the ASNs reference time.

Numerical and experimental tests assess the suitability of the proposed procedure and furnish practical indications on the number of NSNs that can be added in order to preserve the synchronization accuracy.

References

[1] N. Harris, A. Cranny, M. Rivers, K. Smettem, and E. G. Barrett-Lennard, "Application of distributed wireless chloride sensors to environmental monitoring: Initial results," *IEEE Trans. Instrum. Meas.*, vol. 65, no. 4, pp. 736–743, Apr. 2016.

[2] M.-L. Cao, Q.-H. Meng, Y.-Q. Jing, J.-Y. Wang, and M. Zeng, "Distributed sequential location estimation of a gas source via convex combination in WSNs," *IEEE Trans. Instrum. Meas.*, vol. 65, no. 6, pp. 1484–1494, Jun. 2016.

[3] D. Magalotti, P. Placidi, M. Paolucci, A. Scorzoni, and L. Servoli, "Experimental characterization of a wireless personal sensor node for the dosimetry during interventional radiology procedures," *IEEE Trans. Instrum. Meas.*, vol. 65, no. 5, pp. 1070–1078, May 2016.

[4] D. Jayawardana, S. Kharkovsky, R. Liyanapathirana, and X. Zhu, "Measurement system with accelerometer integrated RFID tag for infrastructure health monitoring," *IEEE Trans. Instrum. Meas.*, vol. 65, no. 5, pp. 1163–1171, May 2016.

[5] F. Lamonaca, E. Garone, D. Grimaldi, and A. Nastro, "Localized fine accuracy synchronization in wireless sensor network based on consensus approach," in *Proc. IEEE Int. Instrum. Meas. Technol. Conf. (I2MTC)*, Graz, Austria, May 2012, pp. 2802–2805.

[6] M. Macucci, S. Di Pascoli, P. Marconcini, and B. Tellini, "Derailment detection and data collection in freight trains, based on a wireless sensor network," *IEEE Trans. Instrum. Meas.*, vol. 65, no. 9, pp. 1977–1987, Sep. 2016.

[7] E. Sardini, M. Serpelloni, and V. Pasqui, "Wireless wearable T-shirt for posture monitoring during rehabilitation exercises," *IEEE Trans. Instrum. Meas.*, vol. 64, no. 2, pp. 439–448, Feb. 2015.

[8] F. Lamonaca, A. Gasparri, E. Garone, and D. Grimaldi, "Clock synchronization in wireless sensor network with selective convergence rate for event driven measurement applications," *IEEE Trans. Instrum. Meas.*, vol. 63, no. 9, pp. 2279–2287, Sep. 2014.

[9] A. Mois, T. Sanislav, and S. C. Folea, "A cyber-physical system for environmental monitoring," *IEEE Trans. Instrum. Meas.*, vol. 65, no. 6, pp. 1463–1471, Jun. 2016.

[10] D. Magalotti, P. Placidi, M. Dionigi, A. Scorzoni, and L. Servoli, "Experimental characterization of a personal wireless sensor network for the medical X-ray dosimetry," *IEEE Trans. Instrum. Meas.*, vol. 65, no. 9, pp. 2002–2011, Sep. 2016.

[11] F. Lamonaca, A. Gasparri, and E. Garone, "Wireless sensor networks clock synchronization with selective convergence rate," in *Proc. IFAC Intell. Auto. Veh. Symp. (IAV)*, Gold Coast, QLD, Australia, Jun. 2013, pp. 146–151.

[12] A. Berger, M. Pichler, J. Klinglmayr, A. Potsch, and A. Springer, "Low-complex synchronization algorithms for embedded wireless sensor networks," *IEEE Trans. Instrum. Meas.*, vol. 64, no. 4, pp. 1032–1042, Apr. 2015.

[13] H. Hatime, "Impact of topological characteristics on consensus building in multiagent systems," *IEEE Sensors J.*, vol. 11, no. 12, pp. 3377–3387, Dec. 2011.

[14] L. Chen, G. Carpenter, S. Greenberg, J. Frolik, and X. S. Wang, "An implementation of decentralized consensus building in sensor networks," *IEEE Sensors J.*, vol. 11, no. 3, pp. 667–675, Mar. 2011.

[15] L. Schenato and F. Fiorentin, "Average TimeSynch: A consensus-based protocol for clock synchronization in wireless sensor networks," *Automatica*, vol. 47, no. 9, pp. 1878–1886, Sep. 2011.

[16] L. Moreau, "Stability of multiagent systems with time-dependent communication links," *IEEE Trans. Autom. Control*, vol. 50, no. 2, pp. 169–182, Feb. 2005.

[17] F. Lamonaca, D. Grimaldi, D. L. Carnì, M. Riccio, and A. Nastro, "Preserving synchronization accuracy in slow update wireless sensor network perturbed by plug-in of multi-nodes," in *Proc. IEEE Int. Instrum. Meas. Technol. Conf. (I2MTC)*, Pisa, Italy, May 2015, pp. 1555–1560.

[18] S. Bolognani, R. Carli, E. Lovisari, and S. Zampieri, "A randomized linear algorithm for clock synchronization in multi-agent systems," *IEEE Trans. Autom. Control*, vol. 61, no. 7, pp. 1711–1726, Jul. 2016.

[19] D. Djenouri and M. Bagaa, "Synchronization protocols and implementation issues in wireless sensor networks: A review," *IEEE Syst. J.*, vol. 10, no. 2, pp. 617–627, Jun. 2016.

[20] S. Rahamatkar, *A Light Weight Time Synchronization Approach in Sensor Network: Tree Structured Referencing Time Synchronization Scheme*. Saarbrücken, Germany: LAP Lambert Academic Publishing, 2012, pp. 1–180.

[21] K. S. Yildirim and A. Kantarci, "Time synchronization based on slow-flooding in wireless sensor networks," *IEEE Trans. Parallel Distrib. Syst.*, vol. 25, no. 1, pp. 244–253, Jan. 2014.

[22] H. C. Lee and H. B. Huang, "A low-cost and noninvasive system for the measurement and detection of faulty streetlights," *IEEE Trans. Instrum. Meas.*, vol. 64, no. 4, pp. 1019–1031, Apr. 2015.

[23] B. Ando, S. Baglio, A. Pistorio, G. M. Tina, and C. Ventura, "Sentinella: Smart monitoring of photovoltaic systems at panel level," *IEEE Trans. Instrum. Meas.*, vol. 64, no. 8, pp. 2188–2199, Aug. 2015.

[24] E. Sardini, M. Serpelloni, and M. Lancini, "Wireless instrumented crutches for force and movement measurements for gait monitoring," *IEEE Trans. Instrum. Meas.*, vol. 64, no. 12, pp. 3369–3379, Dec. 2015.

[25] F. Lamonaca and D. Grimaldi, "Synchronization for hot-plugging node in wireless sensor network," in *Proc. IEEE Int. Workshop Meas. Netw. (M&N)*, Naples, Italy, Oct. 2013, pp. 13–18.

[26] F. Lamonaca, D. L. Carnì, and D. Grimaldi, "Time coordination of standalone measurement instruments by synchronized triggering," *Acta Imeko*, vol. 4, no. 3, pp. 23–29, 2015.

[27] E. Garone, A. Gasparri, and F. Lamonaca, "Clock synchronization protocol for wireless sensor networks with bounded communication delays," *Automatica*, vol. 59, pp. 60–72, Sep. 2015.
[28] Y. Fan, Z. Zhang, M. Trinkle, A. D. Dimitrovski, J. B. Song, and H. Li, "A cross-layer defense mechanism against GPS spoofing attacks on PMUs in smart grids," *IEEE Trans. Smart Grid*, vol. 6, no. 6, pp. 2659–2668, Nov. 2015.
[29] E. Garone, A. Gasparri, and F. Lamonaca, "Clock synchronization for wireless sensor network with communication delay," in *Proc. Amer. Control Conf.*, Washington, DC, USA, Jun. 2013, pp. 771–776.
[30] T. Torfs *et al.*, "Low power wireless sensor network for building monitoring," *IEEE Sensors J.*, vol. 13, no. 3, pp. 909–915, Mar. 2013.
[31] M. C. Rodriguez-Sanchez, S. Borromeo, and J. Hernández-Tamames, "Wireless sensor networks for conservation and monitoring cultural assets," *IEEE Sensors J.*, vol. 11, no. 6, pp. 1382–1389, Jun. 2011.
[32] H. C. Lee, Y. M. Fang, B. J. Lee, and C. T. King, "The tube: A rapidly deployable wireless sensor platform for supervising pollution of emergency work," *IEEE Trans. Instrum. Meas.*, vol. 61, no. 10, pp. 2776–2786, Oct. 2012.
[33] H.-C. Lee, A. Banerjee, Y.-M. Fang, B.-J. Lee, and C.-T. King, "Design of a multifunctional wireless sensor for *in-situ* monitoring of debris flows," *IEEE Trans. Instrum. Meas.*, vol. 59, no. 11, pp. 2958–2967, Nov. 2010.
[34] V. Krishnamurthy, K. Fowler, and E. Sazonov, "The effect of time synchronization of wireless sensors on the modal analysis of structures," *Smart Mater. Struct.*, vol. 17, no. 5, p. 055018, 20083.
[35] F. Lamonaca, D. Grimaldi, and R. Morello, "Dynamic scheduling of trigger command for sub-microsecond alignment accuracy in distributed measurement system," *IEEE Transaction Instrum. Meas.*, vol. 63, no. 7, pp. 1795–1803, Jul. 2014.
[36] *Telosb Mote Platform*, Crossbow Technology, Milpitas, CA, USA, 1995.

Francesco Lamonaca (M'11–SM'16) received the M.S. degree in computer science engineering and the Ph.D. degree in computer and system science from the University of Calabria, Rende, Italy, in 2005 and 2010, respectively, and the doctorate equivalent degree in science and engineering science from the Université Libre de Bruxelles, Brussels, Belgium, in 2010 and 2011, respectively.

He is currently an Associate Professor of Electronic Measurements with the University of Sannio, Benevento, Italy. He has authored and co-authored more than 150 papers published in international journals and conference proceedings. His current researches interests include measurement for medical use, characterization of human tissue by thermal analysis, digital signal and image processing for health parameters monitoring, noninvasive monitoring and testing, synchronization of networking measurement instruments and sensors, and distributed measurement systems.

Dr. Lamonaca is a member of the Institute of Electrical and Electronic Engineers (IEEE), the IEEE Society on Instrumentation and Measurement (IM), IEEE IM Technical Committee (TC) 25 "Medical and Biological Measurements," the IEEE IM TC 10 "Waveform Generation, Measurement and Analysis Committee," and the IEEE IM TC 37 "Measurements and Networking," Armed Forces Communications & Electronics Association and Gruppo Misure Elettriche ed Elettroniche (GMEE). He was the special sessions Chair of MeMeA 2016 and organized the special session "smart devices for biomedical applications and health parameters monitoring." He won competitions as first classified: the University of Calabria, the Young Researchers 2010 and 2012; GMEE, mobility research grant 2011; and TE-RE-RD, the Best Paper Awards 2014. He is a Reviewer for international journals and conferences. He organized the special session "synchronization service for measurement and monitoring" at IMEKO TC4, 2014.

Domenico Luca Carnì (M'11) received the master's degree in computer engineering and the Ph.D. degree in systems and computer engineering from the University of Calabria, Rende, Italy, in 2003 and 2006, respectively.

In 2006, he joined the Department of Informatics, Modeling, Electronics and Systems, University of Calabria, as an Assistant Professor of Electric and Electronic Measurements. His current research interests include the measurement on telecommunication systems, characterization of digital to analog and analog to digital converters, digital signal processing for monitoring and testing, virtual instrumentation, and distributed measurement systems.

Maria Riccio (M'11–SM'16) received the master's degree in software engineering, and the Ph.D. degree in information engineering from the University of Sannio, Benevento, Italy, in 2001 and 2010, respectively.

From 2002 to 2010, she was responsible for the research area in Didagroup S.p.A. Since 2010, she has been a Post-Doctoral Researcher of electrical and electronic measurements at the Department of Engineering, University of Sannio. She has authored or co-authored more than 40 papers published in international journals and conference proceedings. She is the owner of some patents. Her current research interests include enhanced learning technologies, wireless sensor network for traffic safety, and body area sensor network for motion-tracking in physical rehabilitation.

She is a member of the Gruppo di Misure Elettriche ed Elettroniche, Institute of Electrical and Electronics Engineers (IEEE), the IEEE Aerospace and Electronic Systems Society, and the IEEE Instrumentation and Measuremente Society. She was the Chair and Organizer of Special Sessions during the IEEE International Symposium on Medical Measurements and Applications of 2016 and 2015. She received the "Best Paper" Award at the Instrumentation and Measurement Technology Conference, 2006-IMTC 2006. She is a Reviewer of international journals and conferences.

Domenico Grimaldi (M'94–SM'10) is a Full Professor of Electronic Measurement with the Department of Computer Sciences, Modeling, Electronics, and System Science, University of Calabria, Rende, Italy, where he has remained in a variety of research and management positions. He is responsible for the Laboratory and for processing the measurement information. He was responsible for the research unit in the frame of the National Projects PRIN, FIRB, and international projects INTERLINK supported by the Italian Ministry for University and Research. He was responsible for the Tempus Project and Leonardo da Vinci Project supported by the European Union, and the PARCO Project supported by Calabria Region. He is the delagate of the Rector of the University of Calabria for the safety. He has authored or co-authored more than 250 papers published in international journals and conference proceedings. His current research interests include the characterization of measurement transducers, digital signal processing for monitoring and testing, distributed measurements and synchronization, and measurement for medical application. The results of his research have led to a number of awards.

Prof. Grimaldi is a member of the Italian Group of Electrical and Electronic Measurements. He is an Associate Editor of IEEE TRANSACTIONS ON INSTRUMENTATION AND MEASUREMENT and of *Metrology and Measurement Systems*.

Gregorio Andria (M'11) was born in Massafra, Italy, in 1956. He received the master's (Hons.) degree in electrical engineering from the State University of Bari, Italy, 1981, and the Ph.D. degree in electrical engineering for power systems, from the Italian Ministry of Education, Rome, Italy, in 1987.

He was engaged as a Research Assistant at the Polytechnic of Bari, Bari, Italy. Since 2001, he has been a Full Professor of Electrical and Electronic Measurements with the Department of Electrical Engineering and Information Technology, Polytechnic of Bari. He currently covers the charges of Rector's Delegate for issues relating to the site of Taranto and of the Dean of the Interdepartmental Center "Magna Grecia," Polytechnic of Bari. His current research interests include electrical and electronic measurements, design and development of advanced sensors, intelligent electronic instrumentation, analysis and measurement of deformed electrical quantities, methods of measurement in electrical drives, environmental and remote sensing measurements, measurements and electronic instrumentation in the biomedical field, measurements and devices for aerospace, and the reliability of measurement and benefits in the statistical quality control devices.